

Anomalous diffusion in QCD matterPaul Caucal^{1,*} and Yacine Mehtar-Tani^{1,2,†}¹*Physics Department, Brookhaven National Laboratory, Upton, New York 11973, USA*²*RIKEN BNL Research Center, Brookhaven National Laboratory, Upton, New York 11973, USA* (Received 12 October 2021; accepted 18 August 2022; published 12 September 2022)

We study the effects of quantum corrections on transverse momentum broadening of a fast parton passing through dense QCD matter. We show that, at leading logarithmic accuracy the broadening distribution tends at late times or equivalently for large system sizes L to a universal distribution that only depends on a single scaling variable k_T^2/Q_s^2 where the typical transverse momentum scale increases with time as $\ln Q_s^2 \simeq (1 + 2\beta) \ln L - \frac{3}{2}(1 + \beta) \ln \ln L$ up to nonuniversal terms, with an anomalous dimension $\beta \sim \sqrt{\alpha_s}$. This property is analogous to geometric scaling of gluon distributions in the saturation regime and traveling-wave solutions to reaction-diffusion processes. We note that since $\beta > 0$ the process is super-diffusive, which is also reflected at large transverse momentum where the scaling distribution exhibits a heavy tail $k_T^{-4+2\beta}$ akin to Lévy random walks.

DOI: [10.1103/PhysRevD.106.L051501](https://doi.org/10.1103/PhysRevD.106.L051501)**I. INTRODUCTION**

Transverse momentum broadening (TMB) of energetic quarks and gluons traversing QCD matter plays a central role in a variety of processes studied at colliders to probe QCD, ranging from jet suppression in heavy-ion collisions [1,2] to transverse-momentum-dependent gluon distribution functions that encode information on the 3D structure of the proton and nuclei in high-energy collisions in particular at small Bjorken x [3–5].

High-energy partons experience random kicks in hot or cold nuclear matter causing their transverse momentum (TM) \mathbf{k}_\perp with respect to their direction of motion to increase over time. The dominant process is given by a single gluon exchange via Coulomb scattering and leads to an approximate Brownian motion in TM space, where the typical TM square scales linearly with system size L , namely $\langle \mathbf{k}_\perp^2 \rangle_{\text{typ}} \sim \hat{q}L$, where \hat{q} is the diffusion coefficient [6–9]. Moreover, radiative processes can also increase the TM of the leading parton due to recoil effects. It has been shown recently that such contributions, albeit suppressed by the coupling constant α_s , are enhanced by double logarithms which must be resummed to all orders when $\alpha_s \ln^2 L \sim 1$ [10–14].

In this paper we go beyond this result by investigating in more detail the consequences of the nonlocal nature of quantum corrections on the TMB distribution. We find in particular that the latter exhibits a universal scaling at large L that we compute analytically along with its subasymptotic deviations exploiting a formal analogy with traveling-wave solutions to reaction-diffusion processes [15–19]. As a consequence of the self-similarity characterizing the anomalous random walk, the TMB distribution is of Lévy type. It is in particular associated with a heavy tail describing rare long steps which extends over a large range of transverse momenta above the typical scale.

Lévy flights are ubiquitous in nature and span a wide variety of stochastic processes in biological systems [20,21], molecular chemistry [22], optical lattice [23], turbulent diffusion and polymer transport theory [24,25]. Furthermore, heavy-tailed distributions are also observed in self-organized critical states [26,27]. In this work, we point out for the first time another occurrence of such random walks in the transport of eikonal partons in dense QCD matter and we compute the anomalous exponents that characterize the deviation from standard diffusion.

II. QUANTUM CORRECTIONS TO TRANSVERSE MOMENTUM BROADENING IN QCD MEDIA

The TMB distribution is related to the forward scattering amplitude $\mathcal{S}(\mathbf{x}_\perp)$ of an effective dipole in the color representation $R = A, F$ with transverse size \mathbf{x}_\perp (see e.g., Refs. [11,28,29]) via a Fourier transform,

$$\mathcal{P}(\mathbf{k}_\perp) = \int d^2\mathbf{x}_\perp e^{-i\mathbf{k}_\perp \cdot \mathbf{x}_\perp} \mathcal{S}(\mathbf{x}_\perp). \quad (1)$$

*pcaucal@bnl.gov

†mehtartani@bnl.gov

Published by the American Physical Society under the terms of the [Creative Commons Attribution 4.0 International license](https://creativecommons.org/licenses/by/4.0/). Further distribution of this work must maintain attribution to the author(s) and the published article's title, journal citation, and DOI. Funded by SCOAP³.

Considering the dipole formulation in position space allows for a straightforward resummation of multiple scattering by exponentiating the single-scattering cross section, so long as the interactions between the dipole and the medium are local. Thus, we may write [30]

$$\mathcal{S}(\mathbf{x}_\perp) = \exp\left(-\frac{1}{4} \frac{C_R}{N_c} \hat{q}(1/x_\perp^2, L) L x_\perp^2\right). \quad (2)$$

The latter relation defines the quenching parameter in the adjoint representation which is assumed to be a slowly varying function of \mathbf{x}_\perp . At tree level it reads $\hat{q}^{(0)}(1/x_\perp^2, L) = \hat{q}_0 \ln(1/(x_\perp^2 \mu^2)) + \mathcal{O}(x_\perp^2 \mu^2)$, up to power-suppressed terms, and is independent of L . For a weakly coupled quark-gluon plasma (QGP) the bare quenching parameter \hat{q}_0 and the infrared transverse scale μ^2 [31] are related to the Debye screening mass in the QGP or to the inverse nucleon size in a nucleus.

It is customary to define the emergent saturation scale $Q_s(L)$ via the relation $\mathcal{S}(x_\perp^2 = 1/Q_s^2(L)) \equiv e^{-1/4}$, or equivalently, $\hat{q}(Q_s^2(L), L)L \equiv Q_s^2(L)$. This definition is standard in small- x physics [34,35], and is also motivated by Molière's theory of multiple scatterings [33,36,37] in which Q_s is the transverse scale that controls the transition between the multiple soft scattering and the single hard scattering regimes. At tree level, one finds approximately $Q_s^2 \sim \hat{q}_0 L \ln(\hat{q}_0 L / \mu^2)$.

Beyond leading order in α_s , one has to account for real and virtual gluon fluctuations in the effective dipole with lifetime τ smaller than the system size. Such fluctuations yield potentially large contributions of the form $\hat{q}^{(1)} \sim \alpha_s \hat{q}^{(0)} \ln^2(L/\tau_0)$ where $\tau_0 \ll L$ is a microscopic scale of order of the mean free path [10]. These radiative corrections to the quenching parameter can be resummed to double logarithmic accuracy (DLA) via an evolution equation ordered in τ [10,12,13,38]:

$$\frac{\partial \hat{q}(\mathbf{k}_\perp^2, \tau)}{\partial \ln \tau} = \int_{Q_s^2(\tau)}^{k_\perp^2} \frac{d\mathbf{k}'_\perp{}^2}{k_\perp'^2} \bar{\alpha}_s \hat{q}(\mathbf{k}'_\perp^2, \tau), \quad (3)$$

$$Q_s^2(\tau) = \hat{q}(Q_s^2(\tau), \tau)\tau, \quad (4)$$

where $\bar{\alpha}_s = \alpha_s N_c / \pi$. The initial condition is the tree-level value $\hat{q}^{(0)}(\mathbf{k}_\perp^2, \tau_0)$. The condition $\mathbf{k}_\perp^2 > Q_s^2(\tau)$ in Eq. (3) ensures that the gluon fluctuations are triggered by a single scattering with plasma constituents whose contribution is logarithmically enhanced compared to the multiple scattering regime for which $\mathbf{k}_\perp^2 \leq Q_s^2(\tau)$. Once Eq. (4) is solved, τ and \mathbf{k}_\perp^2 are fixed by the external parameters L and $1/x_\perp^2$.

In this paper, we address both analytically and numerically the nonlinear system (3) and (4) [39]. Analytic solutions are in general difficult to obtain; however, a solution for the linearized problem that consists in approximating $Q_s^2(\tau) \simeq \hat{q}_0 \tau$ for the emission phase space can be found in Refs. [40,41]. Formally, this linearization is valid

in DLA, which captures all the terms of the form $\bar{\alpha}_s^n Y^{2n}$ where $Y = \ln(L/\tau_0)$, but it misses subleading corrections of the form $\bar{\alpha}_s^n Y^{2n-1} \ln Y$ which are parametrically larger than the single logarithmic ones. This is one of the novelties of the present study, enabling us to highlight the geometric scaling property of transverse momentum diffusion in QCD and to compute its scaling deviations.

III. GEOMETRIC SCALING AND TRAVELING WAVES

The TMB distribution is said to obey geometric scaling if it is only a function of $\mathbf{k}_\perp^2 / Q_s^2(L)$ as a result of scale invariance of the radiative process for large L . Geometric scaling was extensively studied in the context of deep inelastic scattering, where it has been shown that the gluon distribution $g(x, Q^2)$ at small x satisfies this property over a broad region of photon virtuality $-Q^2$ [42–44]. We shall demonstrate that TMB exhibits similar properties.

More precisely, we would have

$$\lim_{L \rightarrow \infty} \hat{q}(\mathbf{k}_\perp^2, L)L = Q_s^2(L) f\left(\ln \frac{\mathbf{k}_\perp^2}{Q_s^2(L)}\right), \quad (5)$$

where f is a function to be determined. By definition we have $\hat{q}(Q_s^2, L)L = Q_s^2$, and thus, $f(0) = 1$. In fact, the nonlinearity of Eq. (3) enforces the evolution to be controlled by a single momentum scale $Q_s(L)$.

Remarkably, it is possible to find the scaling function f for the nonlinear problem defined by Eqs. (3) and (4). In terms of the variables $Y = \ln(L/\tau_0)$ and $\rho = \ln(\mathbf{k}_\perp^2 / (\hat{q}_0 \tau_0))$, the integral equation satisfied by \hat{q} reads

$$\hat{q}(\rho, Y) = \hat{q}^{(0)}(\rho, 0) + \int_0^Y dY' \int_{\rho_s(Y')}^\rho d\rho' \bar{\alpha}_s \hat{q}(\rho', Y'), \quad (6)$$

where $\rho_s(Y) = \ln(Q_s^2(L) / (\hat{q}_0 \tau_0))$. Note that by analyzing the support of the double integral one distinguishes two regimes: if $\rho > \rho_s(Y)$, or $\mathbf{k}_\perp^2 > Q_s^2(L)$, the upper limit of the Y' integral is Y . However, when $\rho \leq \rho_s(Y)$, or $\mathbf{k}_\perp^2 \leq Q_s^2(L)$, the Y' is actually bounded by the scale $Y_s(\rho) < Y$ beyond which the ρ' integral has no support, i.e., $\rho_s(Y_s) \equiv \rho$. In that case, $\hat{q}(\rho, Y) = \hat{q}(\rho, Y_s(\rho))$.

In terms of ρ and Y , the scaling form (5) reads

$$\hat{q}(\rho, Y) = \hat{q}_0 e^{\rho_s(Y) - Y} f(\rho - \rho_s(Y)), \quad (7)$$

which we insert into Eq. (6) and differentiate twice in order to get the second-order equation

$$-\frac{d\rho_s}{dY} f''(x) + \left(\frac{d\rho_s}{dY} - 1\right) f'(x) - \bar{\alpha}_s f(x) = 0, \quad (8)$$

where $x = \rho - \rho_s(Y)$. In order for f to be a function of x only, at large Y , the derivative $d\rho_s/dY$ must converge towards a constant c , which can be interpreted as the speed

of a traveling wave (TW) that propagates to the right on the ρ axis. This is reminiscent of the TW solutions [17] to the Balitsky-Kovchegov (BK) equation [45,46]. The initial conditions set by the saturation boundary read $f(0) = 1$ and $f'(0) = (c - 1)/c$, the latter resulting from $\partial \hat{q}(\rho_s, Y)/\partial Y = 0$. It is then straightforward to solve Eq. (8) with the scaling form $f(x) = e^{\beta x}$ where β is a solution of the quadratic equation $-c\beta^2 + (c - 1)\beta - \bar{\alpha}_s = 0$. We need an additional condition to fully fix the value of the front velocity. This can be done formally by requiring the scaling violations to decay at large Y [see discussion below Eq. (12)]. Physically, the system is driven towards a critical (maximum) slope $\beta = \beta_c$ that corresponds to a minimal velocity that satisfies the additional constraint $dc/d\beta = 0$, provided the initial condition satisfies $\hat{q}^{(0)}(\rho, 0)e^{-\beta \cdot \rho} \rightarrow 0$ at large ρ [18,47], which is the case in the present problem.

As a result we obtain for the minimal velocity $c = 1 + 2\sqrt{\bar{\alpha}_s} + \bar{\alpha}_s^2 + 2\bar{\alpha}_s$ and the solution to Eq. (8) takes the form

$$f(x) = e^{\beta x}(1 + \beta x), \quad \beta \equiv \frac{c - 1}{2c}, \quad (9)$$

where we have dropped the subscript c in β_c for simplicity.

Let us now specify the scaling limit for the two regimes $k_{\perp}^2 \geq Q_s^2(L)$ and $k_{\perp}^2 < Q_s^2(L)$. As discussed below Eq. (6), when $k_{\perp}^2 < Q_s^2(L)$, one has $\hat{q}(\rho, Y) = \hat{q}(\rho, Y_s(\rho))$. Hence, replacing Y by $Y_s(\rho)$ in Eq. (7) and using the fact that $x = \rho - \rho_s(Y_s) = 0$, we readily find $\hat{q}(\rho, Y) = \hat{q}_0 e^{\rho - Y_s(\rho)}$. In the scaling limit, $\rho_s(Y) = cY$ so $Y_s(\rho) = \rho/c$, leading to $\hat{q}(\rho, Y) = \hat{q}_0 e^{2\beta \rho}$ for $\rho < \rho_s(Y)$. In terms of the physical variables the k_{\perp}^2 dependence of \hat{q} that enters the broadening distribution reads, in the large- L limit,

$$\frac{\hat{q}(k_{\perp}^2, L)L}{Q_s^2(L)} = \begin{cases} \left(\frac{k_{\perp}^2}{Q_s^2(L)}\right)^{2\beta} & \text{if } k_{\perp}^2 \leq Q_s^2(L), \\ \left(\frac{k_{\perp}^2}{Q_s^2(L)}\right)^{\beta} \left[1 + \beta \ln\left(\frac{k_{\perp}^2}{Q_s^2(L)}\right)\right] & \text{otherwise,} \end{cases} \quad (10)$$

which is continuous and derivable everywhere. Note that for $\alpha_s \ll 1$, $\beta \simeq \sqrt{\bar{\alpha}_s}$.

To make the interpretation of these results in terms of TWs more transparent we insert Eq. (10) into $\mathcal{S}(x_{\perp})$ and plot the result in Fig. 1 for several values of L . We see that the TW propagates from right to left (from large to small x_T) with increasing L . However, once plotted in terms of $x_T^2 Q_s^2$ as shown in the inset of Fig. 1, they all lie approximately on the same universal curve given by Eqs. (1)–(10). The observed deviations will be discussed in what follows.

We turn now to the calculation of the subasymptotic corrections to the geometric scaling solution (10). Near the wave front, typically for $x \gg 1$, we can look for a solution of the form

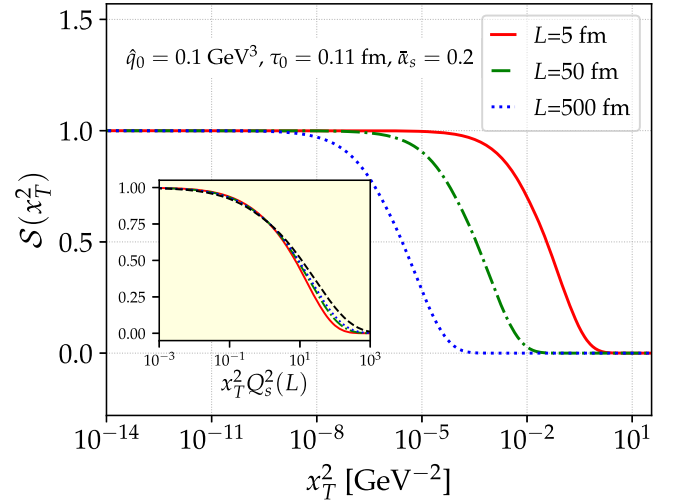


FIG. 1. Dipole scattering amplitude as a function of the transverse dipole size squared x_T^2 for several values of the medium size. The inset shows the same curves as a function of the scaling variable $x_T^2 Q_s^2(L)$ compared to the geometric scaling solution (dashed black).

$$\hat{q}(\rho, Y) = \hat{q}_0 e^{\rho_s(Y) - Y} e^{\beta x} Y^\alpha G\left(\frac{x}{Y^\alpha}\right), \quad (11)$$

$$\rho_s(Y) = cY + b \ln(Y), \quad (12)$$

inspired by the TW ansatz that solves the BK equation [17,48,49] and more generally Fisher-Kolmogorov-Petrovsky-Piskunov (FKPP)-like equations [50,51]. Plugging this ansatz into Eq. (6), one gets a differential equation for $G(z)$. Because the coefficient of Y and Y^α (assuming $\alpha > 0$) in this equation must vanish, we recover the two previous constraints that fix the values of c and β . Then, neglecting the power-suppressed terms Y^{-1} and $Y^{-\alpha-1}$, one finds $-cY^{-\alpha}G''(z) - \beta\alpha z Y^{\alpha-1}G'(z) + \beta(-b\beta + b + \alpha)Y^{\alpha-1}G(z) = 0$. The homogeneity condition implies that the coefficient α must be equal to $1/2$ so that the deviation from the scaling form near the wave front grows in a diffusive way as Y increases.

The differential equation for G is solved with the initial condition $G(z) \sim \beta z$ at small z , in order to match with the scaling limit f . Similarly to the FKPP or BK equations, the boundary conditions at $z = \infty$ [52] constrain the value of the coefficient b to be [18,47,48]

$$b = -\frac{3}{2(1-\beta)}. \quad (13)$$

This yields the solution

$$G(z = x/\sqrt{Y}) = \beta z \exp\left(-\frac{\beta z^2}{4c}\right). \quad (14)$$

The value of b we extract from this analysis is novel and a consequence of the nonlinearity of the saturation boundary. In the linearized problem with the lower bound in the integral of Eq. (6) set to Y instead of $\rho_s(Y)$, one gets

$b = -3/2$ [40], whereas in the nonlinear case, we have $b \simeq -3/2(1 + \sqrt{\bar{\alpha}_s})$ for $\alpha_s \ll 1$. The subleading term provides a correction to the saturation line which is parametrically of order $\sqrt{\bar{\alpha}_s} \ln Y$ and therefore dominates over the single logarithmic corrections of order $\bar{\alpha}_s Y \sim \sqrt{\bar{\alpha}_s}$ since in DLA $Y \sim 1/\sqrt{\bar{\alpha}_s} \gg 1$.

The TW solution (14) provides the functional form of $\hat{q}(\rho, Y)$ near the wave front, i.e., for $x = \rho - \rho_s(Y) \sim \sqrt{Y} \gg 1$ and fixes the value of the coefficient b in the asymptotic expansion of $\rho_s(Y)$. For small values of x , one can find the scaling deviations by looking for a solution as a power series in $1/\sqrt{Y}$ of the form $\hat{q}(\rho, Y) = \hat{q}_0 e^{\rho_s(Y)-Y} e^{\beta x} \sum_{n \geq 0} Y^{-n/2} H_n(x)$ [18]. Plugging this form into Eq. (6) gives second-order differential equations for $H_1(x)$ and $H_2(x)$, whose initial conditions are constrained by the definition of Q_s . The solutions to these equations read $H_1(x) = 0$ and $H_2(x) = bx/c^2 [1 + (c-1)(c+3)/(8c)x + (c-1)^2(1+c)/(48c^2)x^2]$ [39]. The last term in this expression is included in the solution (14), as can be checked by expanding the function G for large Y , but not the first two since Eq. (14) is only valid at large x . Combining the scaling limit with its deviation provided by the function G for $x \sim \sqrt{Y}$ and $H_2(x)$ for all x up to powers of $Y^{-3/2}$, our final result reads

$$\frac{\hat{q}(\mathbf{k}_\perp^2, L)L}{Q_s^2(L)} = \exp\left(\beta x - \frac{\beta x^2}{4cY}\right) \left[1 + \beta x + \frac{bx}{c^2 Y} \left(1 + \frac{\beta(c+4)x}{6} \right) + \mathcal{O}(Y^{-3/2}) \right], \quad (15)$$

with $x = \ln(\mathbf{k}_\perp^2/Q_s^2(L))$, $Y = \ln(L/\tau_0)$, and $\ln(Q_s^2(L)/(\hat{q}_0\tau_0))$ given by Eq. (12).

This solution is independent of the initial condition (for physically relevant ones), and only depends on the value of $\bar{\alpha}_s$ via the coefficients c , β and b . The resummed TMB distribution displays a universal behavior independent of the nonperturbative modeling of the tree-level distribution often used as an initial condition for nonlinear small- x evolution [53,54]. It can therefore provide a model-independent functional form for the initial condition of the BK equation, that includes gluon fluctuations enhanced by double logs, $\bar{\alpha}_s \ln^2 A^{1/3}$, inside the nucleus target to all orders.

IV. SUPER-DIFFUSION AND MODIFICATION OF RUTHERFORD SCATTERING

In this section, we investigate the physical consequences of the scaling solution (10) for $\hat{q}(\mathbf{k}_\perp^2, L)$ on the TMB distribution given by Eq. (1), in particular at large k_T , where the distribution is characterized by rare events that are sensitive to the point-like nature of the medium scattering centers [55,56]. In Fig. 2, we plot the TMB distribution $\mathcal{P}(\mathbf{k}_\perp)$ as a function of $k_T/Q_s(L)$ with $Y = \ln(L/\tau_0) = 4$, for the following setups: (i) tree level, in dash-dotted grey, (ii) after quantum evolution obtained by solving Eq. (4)

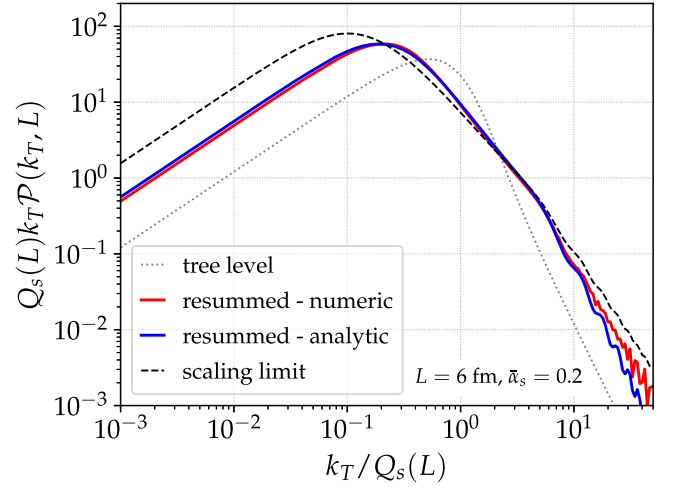


FIG. 2. TMB distribution of a high-energy gluon propagating through a dense medium of size L at tree level (dotted line) and after resummation of the leading radiative corrections (solid red). The dashed black line is the scaling limit when $L \rightarrow \infty$ and the blue curve is our analytic result given by Eq. (15) including subasymptotic corrections.

numerically, in red, (iii) in blue, using the expression (15) that includes subasymptotic corrections to the scaling limit, and (iv) finally, in dashed black, the scaling limit $Y \rightarrow \infty$ of Eq. (15). Interestingly, the universal subasymptotic corrections account for the relatively large deviations between the asymptotic curve and the exact numerical result at the moderate value of $L = 6$ fm.

The k_T distribution exhibits two different regimes: the region of the peak, near $Q_s(L)$ and the large- k_T tail, with $k_T \gg Q_s(L)$. These results can be interpreted in terms of a special kind of random walk (here in momentum space) called Lévy flight. Such a remarkable connection with statistical physics enables us to highlight some interesting features: (i) self-similar dynamics, (ii) super-diffusion, and (iii) a power-law tail with slower decay than the Rutherford k_\perp^{-4} behavior seen at tree level.

In order to further the connection with the physics of anomalous diffusion, consider the scaling limit of the TMB distribution in the vicinity of the peak where the shape of the distribution is controlled by the first line in Eq. (10). Using this solution, one finds that $\mathcal{S}(\mathbf{x}_\perp) \simeq \exp[-\frac{1}{4} \frac{C_R}{N_c} (|\mathbf{x}_\perp| Q_s)^{2-4\beta}]$. In momentum space, it implies that the distribution $\mathcal{P}(\mathbf{k}_\perp)$ satisfies a generalized Fokker-Planck equation, $\partial \mathcal{P} / \partial L \propto -(-\Delta)^{1-2\beta} \mathcal{P}$, where the so-called fractional Laplace operator $(-\Delta)^{\gamma/2}$ is defined by its Fourier transform $|\mathbf{x}_\perp|^\gamma$ [57,58]. This fractional diffusion equation (without external potential) is satisfied by the probability density for the position of a particle undergoing a Lévy flight process in two dimensions [59] with stability index $\gamma = 2-4\beta \simeq 2 - 4\sqrt{\bar{\alpha}_s} + \mathcal{O}(\alpha_s)$.

Because of its heavy tail (to be discussed thereafter), the mean k_T^2 of the TMB distribution is not defined.

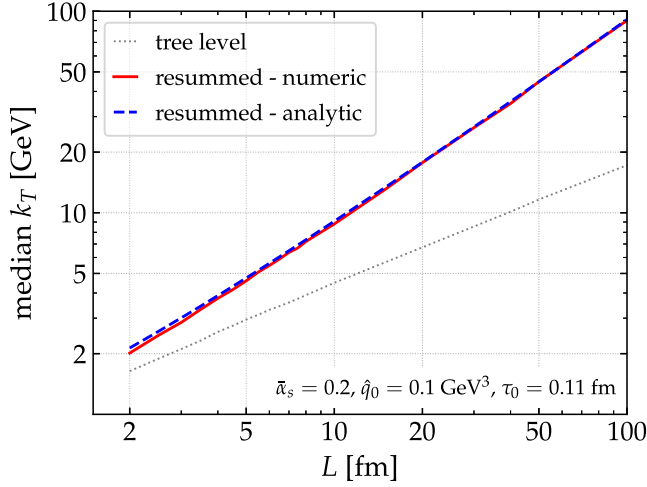


FIG. 3. System size dependence of the median of the TMB distribution at tree level (dotted line) and after numerical resummation of radiative corrections (red line). The dashed blue line is our analytic prediction given by Eq. (12).

Nevertheless, it is possible to introduce a measure of the characteristic width of the k_T distribution, and study its behavior as a function of the medium size L . In what follows, we shall use the median value $\langle k_T \rangle_{\text{med}}$ of $k_T \mathcal{P}(k_T)$ which is shown in Fig. 3 for three different scenarios. The grey dotted curve, shows the tree-level result. In this case, the median scales approximately like $(L \ln L)^{1/2}$, which up to the logarithmic factor resulting from the Coulomb logarithm in the initial condition, exhibits the standard diffusion scaling. The red line is the median of the k_T distribution obtained using the resummed value of \hat{q} with fixed coupling, after numerical resolution of Eq. (4). We then compare this result with our analytic prediction (12) (assuming $\langle k_T \rangle_{\text{med}} \propto Q_s$ [60]), $\langle k_T \rangle_{\text{med}} \propto L^{\frac{c}{2} + \frac{\ln(Y)}{2Y}}$, which is represented in blue in Fig. 3. Remarkably, the agreement is excellent down to rather small values of $L \sim 3$ fm. We have also checked that our asymptotic expansion for ρ_s matches the numerical simulations down to $Y \sim 4$ with $\mathcal{O}(5\%)$ accuracy. Since $c/2 > 1/2$, the median grows faster than \sqrt{L} at large L , illustrating the super-diffusive behavior of TMB beyond leading order, with a deviation to the standard diffusion of order $\sqrt{\bar{\alpha}_s}$.

Another important aspect of Lévy flights is the power-law decay of the step-length distribution for a Lévy walker [61,62]. This reflects the fact that long jumps with arbitrary length may occur with non-negligible probability. In the problem at hand, this power-law tail can also be understood as a consequence of the self-similar nature of overlapping successive gluon fluctuations. The tail of the TMB distribution is controlled by the large- k_{\perp}^2 behavior of $\hat{q}(k_{\perp}^2, L)$, and consequently, by the exponential in the second line of Eq. (10). Note, however, that the scaling limit encompasses two stability indices: one controlling the peak and the median, as discussed above, and one controlling the tail of

the distribution [cf. Eq. (10)]. Without loss of generality, one can derive the leading behavior of $\mathcal{P}(k_{\perp})$ at large k_T by expanding the dipole S matrix for small dipole sizes and then expanding the x_{\perp} integrant assuming $\ln(k_{\perp}^2/(\hat{q}_0 L)) \gg \ln(1/(x_{\perp}^2 k_{\perp}^2)) \sim 1$ since x_{\perp} and k_{\perp} are conjugate to one another and k_T is large. As a result the Fourier transform can be approximated by [39]

$$\mathcal{P}(k_{\perp}) \underset{k_T \rightarrow \infty}{\sim} \bar{\nabla}_{k_{\perp}}^2 \frac{\pi}{k_{\perp}^2} \frac{d\hat{q}(k_{\perp}^2, L)L}{d \ln k_{\perp}^2}, \quad (16)$$

up to logarithmically suppressed terms. This formula quantifies the deviations from the Rutherford scattering cross section that are induced by radiative corrections. Applying Eq. (16) to our scaling solution (10), one finds the tail

$$\mathcal{P}(k_{\perp}) \underset{k_T \rightarrow \infty}{\propto} \frac{1}{Q_s^2(L)} \left(\frac{Q_s^2(L)}{k_{\perp}^2} \right)^{\nu}, \quad (17)$$

with $\nu = 2 - \beta + \mathcal{O}(\ln(x)/x)$. The corrections to the power-law behavior are due to the prefactor in the second line of Eq. (10). The power of the tail deviates from the tree-level Rutherford $\nu = 2$ behavior by $\sim -2\sqrt{\bar{\alpha}_s}$. The form of ν is correct in the strict scaling limit $L \rightarrow \infty$. For finite L values, the $1/k_{\perp}^4$ tail is recovered at very large k_T , as can be inferred from the linearized analytic solution [40] which yields $\nu = 2 - 2\sqrt{\bar{\alpha}_s} Y/x$ (when $x \gg Y$). The fact that geometric scaling extends into the tail region is known in the context of saturation physics as the “extended geometric scaling window” corresponding to $Q_s \ll k_T \ll Q_s^2/\mu$.

V. SUMMARY

In summary, we have studied the transverse momentum distribution of a high-energy parton propagating through a dense QCD medium, including resummation of radiative corrections within a modified double-logarithmic approximation which accounts for the nonlinear dynamics due to multiple scatterings that restrict the phase space for quantum fluctuations. We have found that the nonlinearity and self-similarity of overlapping multiple gluon radiations lead to a universal scaling limit at large system sizes, which exhibits a super-diffusive regime and a power-law decay akin to Lévy flights. Although at very high k_T , the distribution is characterized by point-like interactions of Rutherford type, for moderately large k_T we observed a weaker power due to the nonlocal nature of the interactions which is the hallmark of scale-invariant phenomena.

Concerning phenomenological applications, we point out the relevance of our analytic solutions in the study of nuclear structure at high energy as it provides a new initial condition for nonlinear evolution of the gluon distribution. We leave for future work the question of the experimental detection of this emergent QCD phenomenon in heavy-ion collisions as well as running coupling corrections which are expected to yield mild scaling violations.

ACKNOWLEDGMENTS

This work was supported by the U.S. Department of Energy, Office of Science, Office of Nuclear Physics, under contract No. DE-SC0012704. Y.M.-T.

acknowledges support from the Relativistic Heavy Ion Collider (RHIC) Physics Fellow Program of the RIKEN Brookhaven National Laboratory (BNL) Research Center.

-
- [1] J.-P. Blaizot and Y. Mehtar-Tani, *Int. J. Mod. Phys. E* **24**, 1530012 (2015).
- [2] G.-Y. Qin and X.-N. Wang, *Int. J. Mod. Phys. E* **24**, 1530014 (2015).
- [3] L. N. Lipatov, *Phys. Rep.* **286**, 131 (1997).
- [4] F. Gelis, E. Iancu, J. Jalilian-Marian, and R. Venugopalan, *Annu. Rev. Nucl. Part. Sci.* **60**, 463 (2010).
- [5] J. L. Albacete and C. Marquet, *Prog. Part. Nucl. Phys.* **76**, 1 (2014).
- [6] R. Baier, Y. L. Dokshitzer, A. H. Mueller, S. Peigne, and D. Schiff, *Nucl. Phys.* **B484**, 265 (1997).
- [7] B. G. Zakharov, *JETP Lett.* **63**, 952 (1996).
- [8] R. Baier, Y. L. Dokshitzer, A. H. Mueller, S. Peigne, and D. Schiff, *Nucl. Phys.* **B483**, 291 (1997).
- [9] B. G. Zakharov, *JETP Lett.* **65**, 615 (1997).
- [10] T. Liou, A. H. Mueller, and B. Wu, *Nucl. Phys.* **A916**, 102 (2013).
- [11] J.-P. Blaizot, F. Dominguez, E. Iancu, and Y. Mehtar-Tani, *J. High Energy Phys.* **06** (2014) 075.
- [12] J.-P. Blaizot and Y. Mehtar-Tani, *Nucl. Phys.* **A929**, 202 (2014).
- [13] E. Iancu, *J. High Energy Phys.* **10** (2014) 095.
- [14] E. Iancu, P. Taels, and B. Wu, *Phys. Lett. B* **786**, 288 (2018).
- [15] G. Dee and J. Langer, *Phys. Rev. Lett.* **50**, 383 (1983).
- [16] W. Van Saarloos, *Phys. Rev. Lett.* **58**, 2571 (1987).
- [17] S. Munier and R. B. Peschanski, *Phys. Rev. Lett.* **91**, 232001 (2003).
- [18] U. Ebert and W. van Saarloos, *Physica (Amsterdam)* **146D**, 199 (2000).
- [19] W. Van Saarloos, *Phys. Rep.* **386**, 29222 (2003).
- [20] G. M. Viswanathan, V. Afanasyev, S. V. Buldyrev, E. Murphy, P. Prince, and H. E. Stanley, *Nature (London)* **381**, 413 (1996).
- [21] A. M. Edwards, R. A. Phillips, N. W. Watkins, M. P. Freeman, E. J. Murphy, V. Afanasyev, S. V. Buldyrev, M. G. da Luz, E. P. Raposo, H. E. Stanley *et al.*, *Nature (London)* **449**, 1044 (2007).
- [22] G. Zumofen and J. Klafter, *Chem. Phys. Lett.* **219**, 303 (1994).
- [23] H. Katori, S. Schlipf, and H. Walther, *Phys. Rev. Lett.* **79**, 2221 (1997).
- [24] M. F. Shlesinger, G. M. Zaslavsky, and J. Klafter, *Nature (London)* **363**, 31 (1993).
- [25] M. F. Shlesinger, G. M. Zaslavsky, and U. Frisch, *Lévy Flights and Related Topics in Physics* (Springer Berlin, Heidelberg, 1995), Vol. 450, 10.1007/3-540-59222-9.
- [26] P. Bak, C. Tang, and K. Wiesenfeld, *Phys. Rev. Lett.* **59**, 381 (1987).
- [27] P. Bak, C. Tang, and K. Wiesenfeld, *Phys. Rev. A* **38**, 364 (1988).
- [28] Y. V. Kovchegov and E. Levin, *Quantum Chromodynamics at High Energy* (Cambridge University Press, Cambridge, England, 2012), Vol. 33.
- [29] F. D’Eramo, H. Liu, and K. Rajagopal, *Phys. Rev. D* **84**, 065015 (2011).
- [30] We use bold type for two dimensional transverse vectors and note $a_T = |\mathbf{a}_\perp|$.
- [31] μ^2 can be obtained from the hard thermal loop value of the collision rate [32]. They read respectively $\hat{q}_0 = \alpha_s N_c m_D^2 T$ and $\mu = m_D e^{-1+\gamma_E}/2$ [33], with T the plasma temperature, m_D the Debye mass. In our numerical results, we fix \hat{q}_0 to 0.1 GeV³ and $\tau_0 = e\mu^2/\hat{q}_0$ to 0.11 fm.
- [32] P. Aurenche, F. Gelis, and H. Zaraket, *J. High Energy Phys.* **05** (2002) 043.
- [33] J. a. Barata, Y. Mehtar-Tani, A. Soto-Ontoso, and K. Tywoniuk, *Phys. Rev. D* **104**, 054047 (2021).
- [34] H. Kowalski and D. Teaney, *Phys. Rev. D* **68**, 114005 (2003).
- [35] T. Lappi, *Phys. Lett. B* **703**, 325 (2011).
- [36] G. Moliere, *Z. Naturforsch.* **3A**, 78 (1948).
- [37] H. A. Bethe, *Phys. Rev.* **89**, 1256 (1953).
- [38] J.-P. Blaizot and F. Dominguez, *Phys. Rev. D* **99**, 054005 (2019).
- [39] See Supplemental Material at <http://link.aps.org/supplemental/10.1103/PhysRevD.106.L051501> for more details about the numerical resolution of Eqs. (3) and (4) (the evolution equation is solved after discretization using the Euler method), the calculation of the sub-asymptotic corrections away from the wave front and the calculation of the large k_T tail of the TMB distribution.
- [40] E. Iancu and D. N. Triantafyllopoulos, *Phys. Rev. D* **90**, 074002 (2014).
- [41] A. H. Mueller, B. Wu, B.-W. Xiao, and F. Yuan, *Phys. Rev. D* **95**, 034007 (2017).
- [42] A. M. Stasto, K. J. Golec-Biernat, and J. Kwiecinski, *Phys. Rev. Lett.* **86**, 596 (2001).
- [43] E. Iancu, K. Itakura, and L. McLerran, *Nucl. Phys.* **A708**, 327 (2002).
- [44] J. Kwiecinski and A. M. Stasto, *Phys. Rev. D* **66**, 014013 (2002).
- [45] I. Balitsky, *Nucl. Phys.* **B463**, 99 (1996).
- [46] Y. V. Kovchegov, *Phys. Rev. D* **60**, 034008 (1999).
- [47] E. Brunet and B. Derrida, *Phys. Rev. E* **56**, 2597 (1997).
- [48] S. Munier and R. B. Peschanski, *Phys. Rev. D* **69**, 034008 (2004).
- [49] S. Munier and R. B. Peschanski, *Phys. Rev. D* **70**, 077503 (2004).

- [50] R. A. Fisher, *Ann. Eugen.* **7**, 355 (1937).
- [51] A. N. Kolmogorov, *Bull. Univ. Moskow, Ser. Internat., Sec. A* **1**, 1 (1937).
- [52] G must decay faster than a power law and be positive 2000.
- [53] L. D. McLerran and R. Venugopalan, *Phys. Rev. D* **49**, 2233 (1994).
- [54] L. D. McLerran and R. Venugopalan, *Phys. Rev. D* **49**, 3352 (1994).
- [55] F. D'Eramo, M. Lekaveckas, H. Liu, and K. Rajagopal, *J. High Energy Phys.* **05** (2013) 031.
- [56] F. D'Eramo, K. Rajagopal, and Y. Yin, *J. High Energy Phys.* **01** (2019) 172.
- [57] R. Hilfer, Threefold introduction to fractional derivatives, in *Anomalous Transport* (John Wiley & Sons, Ltd), Chap. 2, pp. 17–73.
- [58] M. Kwaśnicki, *Fract. Calc. Appl. Anal.* **20**, 7 (2017).
- [59] A. A. Dubkov, B. Spagnolo, and V. V. Uchaikin, *Int. J. Bifurcation Chaos Appl. Sci. Eng.* **18**, 2649 (2008).
- [60] The unknown pre-factor is determined by a fit to the numerical result at large L .
- [61] J. Klafter, A. Blumen, and M. F. Shlesinger, *Phys. Rev. A* **35**, 3081 (1987).
- [62] R. Metzler, E. Barkai, and J. Klafter, *Europhys. Lett.* **46**, 431 (1999).